# Resonances in Nonaxisymmetric Gravitational Potentials

Bruno Sicardy[iD]
LESIA, Observatoire de Paris, Sorbonne Université, Université PSL, CNRS, Univ. Paris Diderot, Sorbonne Paris Cité, 5 place Jules Janssen, F-92195 Meudon,
France; bruno.sicardy@obspm.fr

## Abstract

We study sectoral resonances of the form $j\kappa = m(n - \Omega)$ around a nonaxisymmetric body with spin rate $\Omega$, where $\kappa$ and $n$ are the epicyclic frequency and mean motion of a particle, respectively, where $j > 0$ and $m$ ($<0$ or $>0$) are integers, $j$ being the order of the resonance. This describes $n/\Omega \sim m/(m - j)$ resonances inside and outside the corotation radius, as well as prograde and retrograde resonances. Results are as follows: (1) the kinematics of a periodic orbit depends only on $(m', j')$, the irreducible (relatively prime) version of $(m, j)$. In a rotating frame, the periodic orbit has $j'$ braids, $|m'|$ identical sectors, and $|m'|(j' - 1)$ self-crossing points; (2) thus, Lindblad resonances (with $j = 1$) are free of self-crossing points; (3) resonances with the same $j'$ and opposite $m'$ have the same kinematics, and are called *twins*; (4) the order of a resonance at a given $n/\Omega$ depends on the symmetry of the potential. A potential that is invariant under a $2\pi/k$-rotation creates only resonances with $m$ multiple of $k$; (5) resonances with the same $j$ and opposite $m$ have the same kinematics and same dynamics, and are called *true twins*; (6) A retrograde resonance ($n/\Omega < 0$) is always of higher order than its prograde counterpart ($n/\Omega > 0$); (7) the resonance strengths can be calculated in a compact form with the classical operators used in the case of a perturbing satellite. Applications to Chariklo and Haumea are made.

*Unified Astronomy Thesaurus concepts:* Galaxy disks (589); Orbital resonances (1181); Planetary rings (1254); Minor planets (1065); Centaurs (215); Trans-Neptunian objects (1705); Gravitational interaction (669)

## 1. Introduction

Resonances between a nonaxisymmetric rotating potential and orbiting particles have a very vast domain of applications, from galactic disks perturbed by a central bar to spiral waves excited in Saturn's rings by satellites or planetary modes. More recent examples are given by dense rings discovered around the small Centaur object Chariklo in 2013 (Braga-Ribas et al. 2014), and the trans-Neptunian dwarf planet Haumea in 2017 (Ortiz et al. 2017). Both objects significantly depart from axisymmetric shapes, and are thus expected to drive strong resonances in their respective circumbody collisional disks (Sicardy et al. 2019, 2020).

For a better understanding of these disks, it is important to clarify and classify the kinematics and dynamics of the various resonant orbits. Also, considering the variety of shapes assumed by those bodies, a simple numerical scheme to calculate the resonance strengths is desirable. In the case of a perturbing satellite, resonance strengths are classically calculated by using operators (denoted $F_n$ in this paper) acting on Laplace coefficients. Those operators can be found in various publications, see, for instance, Murray & Dermott (2000) and Ellis & Murray (2000), MD00/EM00 herein. Here I show that the $F_n$ operators can in fact be used formally for any nonaxisymmetric potential, provided that some symmetry conditions are met. Those operators encapsulate in a single expression the direct and indirect terms of the potential, as well as inner and outer resonances (lying inside and outside the corotation radius, respectively), and account for both prograde or retrograde particle motions.

This paper is organized as follows: Section 2 provides the general context of the study, Section 3 classifies the various resonances that occur in that context, Section 4 describes the structure of the resonant orbits (kinematics and dynamics), Section 5 shows how the $F_n$ operators mentioned above can be

used for a generic potential, with applications to Chariklo and Haumea, assumed to be homogeneous triaxial ellipsoids. Section 6 provides concluding remarks.

## 2. Preliminay Remarks

We consider a body rotating at constant angular speed $\Omega = 2\pi/T_{\rm rot}$, where $T_{\rm rot}$ is the rotation period. The following simplifying assumptions are made:

(i) The body rotates around one if its principal axes of inertia, i.e., without wobbling motion.
(ii) The mass distribution of the body is symmetrical with respect to a plane perpendicular to the rotation axis, called the equatorial plane.
(iii) The mass distribution possesses a plane of symmetry that contains the rotation axis.

An example is a spherical object with a mass anomaly sitting at its equator. Another example is a triaxial homogeneous ellipsoid rotating around its smallest axis. Further examples are given by sectoral resonances stemming for normal modes in a gaseous planet.[1]

The time-averaged gravitational potential created by the body is axisymmetric. From hypothesis (i), the average vertical angular momentum (the component that is parallel to the rotation axis) of the orbiting particles is conserved. Consequently, a dissipative collisional set of particles surrounding the body settles into the equatorial plane, as this configuration minimizes energy for a constant vertical angular momentum. From hypothesis (ii), no vertical forces are exerted on the equatorial disk, so that no vertical resonances will be considered here.

---

[1] This is a particular case of tesseral resonances, where the potential depends only on longitude, not latitude.

Notations are classical: the position vector $\boldsymbol{r}$ of a particle in the equatorial plane (counted from the center of mass of the body) is expressed in polar coordinates $(r, L)$, where $r = \|\boldsymbol{r}\|$ and $L$ is the true longitude counted from an arbitrary origin. The orientation of the body is measured by the longitude $\lambda' = \Omega t$ of a reference point on its equator, $t$ being the time. The motion of the particle is described by its Keplerian orbital elements $a$, $e$, $\lambda$, $\varpi$, i.e., the semimajor axis, orbital eccentricity, mean longitude, and longitude of pericenter, respectively.

In an inertial frame, a particle is submitted to a time-dependent potential. From hypotheses (i) and (ii), this potential takes the form $U(r, \theta)$, where $\theta = L - \lambda' = L - \Omega t$. This time-dependence is eliminated by writing the equations of motion in the frame corotating with the body. In that frame, the energy of the particle is a constant of motion, called the Jacobi constant. As it moves in the equatorial plane, the particle has two degrees of freedom, each associated with a fundamental frequency. One is the radial epicyclic frequency $\kappa = n - \dot{\varpi}$ (where the dot denotes time derivative), the frequency at which the particle returns to its pericenter, and the other is the synodic frequency $n - \Omega$, the frequency at which the particle returns to a fixed position relative to the body.

As $U(r, \theta)$ is $2\pi$-periodic in $\theta$, it can be Fourier-expanded as $U(\boldsymbol{r}) = \sum_{m=0}^{+\infty} U_m(r)\cos(m\theta + \varphi_m)$, where $U_m$ and $\varphi_m$ are uniquely defined. From hypothesis (iii), $U(r, \theta)$ is an even function of $\theta$ if the reference point on the body is taken in the vertical plane of symmetry. Then $\varphi_m = 0$ and

$$U(\boldsymbol{r}) = \sum_{m=0}^{+\infty} U_m(r)\cos(m\theta). \qquad (1)$$

Here, the integer $m$ is called the *azimuthal number*. It describes the number of cycles completed by the potential during one revolution around the body. A more symmetric form can be adopted, in which $m$ assumes both positive and negative values,

$$U(\boldsymbol{r}) = \sum_{m=-\infty}^{+\infty} U_m(r)\cos(m\theta), \text{ with } U_{(-m)} = U_{(m)}, \qquad (2)$$

the parity condition ensuring the unicity of the coefficients $U_m(r)$. In this case, each coefficient $U_m(r)$ is divided by two compared to its value in Equation (2) (except for $U_0(r)$, which remains unchanged). Choosing between Equations (1) and (2) is arbitrary. Here I choose Equation (2) as it offers a more natural way to expand the potential in resonant terms, see Section 4.

## 3. Resonance Taxonomy

The potential $U(r, \theta)$ can be Fourier-expanded along linear combinations of the fundamental frequencies $\kappa$ and $n - \Omega$,

$$\nu_{j,m} = j\kappa - m(n - \Omega), \qquad (3)$$

where $m$ can be positive or negative, see above. Without loss of generality, the integer $j$ can be taken as always positive. It is the order of the resonance, see Section 4.1. Resonances occur for $\nu_{j,m} = 0$. If $j = 0$ then

$$n = \Omega, \qquad (4)$$

called the corotation resonance. This resonance is discussed in the context of elongated bodies by Scheeres (1994) and Sicardy et al. (2019) and will not be considered further here. Thus, we

restrict ourselves to the case $j > 0$, and the resonance condition reads

$$j\kappa = m(n - \Omega). \qquad (5)$$

This means that after $|m|$ radial oscillations, the particle completes exactly $j$ synodic period around the body. This excites the orbital eccentricity of the particles, a way to create a coupling between the disk and the body. From $\dot{\varpi} = n - \kappa$, Equation (5) can be re-expressed as

$$\frac{n - \dot{\varpi}}{\Omega - \dot{\varpi}} = \frac{m}{m - j}, \qquad (6)$$

meaning that in a frame rotating at the particle precession rate $\dot{\varpi}$, the particle completes $m$ revolutions while the body completes $m - j$ rotations, hence the notation "$m/(m - j)$" resonance.[2] The case $m = j$ corresponds to the apsidal resonance $\Omega = \dot{\varpi}$, in which the particle's orbit precesses at the rotation rate of the body. For moderately nonaxisymmetric potentials, we have $\dot{\varpi} \ll \Omega$, so that apsidal resonances do not occur and this case is not studied here. Equation (6) can then be written

$$\frac{n}{\Omega} \sim \frac{m}{m - j}. \qquad (7)$$

### 3.1. Location of Resonances

The axisymmetric part of the potential (the term $U_0(r)$ in Equation (2)) provides $n$ and $\kappa$ (Chandrasekhar 1942):

$$n^2(r) = \frac{1}{r}\frac{dU_0(r)}{dr} \text{ and } \kappa^2(r) = \frac{1}{r^3}\frac{d(r^4 n^2)}{dr}. \qquad (8)$$

The condition $j\kappa = m(n - \Omega)$ then allows the calculation of the resonance location, see a practical example in Section 5.

### 3.2. Prograde and Retrograde Resonances

A debris disk around a body may result from an impact, so that rings may move in two opposite directions, prograde or retrograde.[3] Retrograde resonances then occur for $n/\Omega \sim m/(m - j) < 0$. As $j > 0$, this occurs for

$$0 < m < j, \qquad (9)$$

while prograde resonances occur for

$$m < 0 \text{ or } j < m. \qquad (10)$$

Note in passing that in Equation (5), $\kappa$ and $n$ must have the same sign in order to consistently describe a progade or retrograde motion. Adopting arbitrarily $\Omega > 0$, a prograde orbit has $\kappa, n > 0$, while a retrograde orbit has $\kappa, n < 0$.

### 3.3. Inner and Outer Resonances

The position of a resonance can be interior to the corotation radius (where $n = \Omega$), in which case we talk about an inner (or internal) resonance, and $|n/\Omega| > 1$. If the resonance occurs

---

[2] In galactic dynamics, $\kappa$ and $\Omega$ are usually very different so that this approximation does not hold, and the notation $m/(m - j)$ resonance is meaningless. Instead, the cases corresponding to $j = 1$ are sometimes referred to as a $m : 1$ (Lindblad) resonance, see, e.g., Pfenniger (1984).

[3] Retrograde motions may also be encountered with exoplanets orbiting a circular binary stellar system, see Morais & Giuppone (2012).
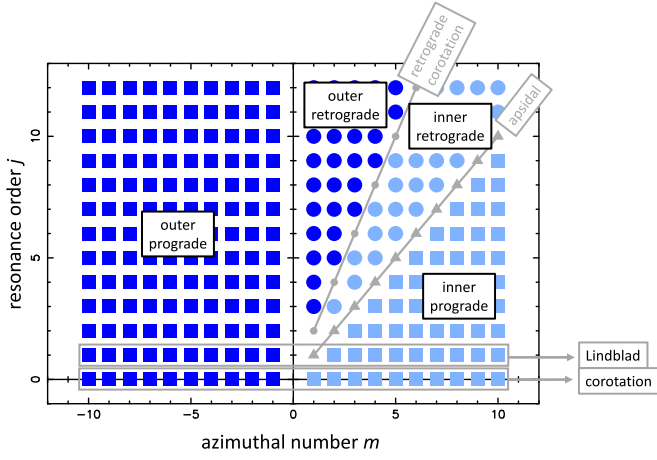
**Figure 1.** Resonance taxonomy in a $(m, j)$ diagram, where $m$ is the azimuthal number and $j$ is the resonance order. Squares (resp. dots) are for prograde (resp. retrograde) resonances. Darker (resp. lighter) blue is for outer (resp. inner) resonances. Gray triangles are for apsidal resonances (not treated here). Dots are for the retrograde corotation.

outside the corotation radius, we talk about an outer (or external) resonance, and $|n/\Omega| < 1$. From Equation (7), resonances with $m < 0$ are always external. For $0 < j < 2m$, the resonances are internal and for $2m < j$, they are external. The case $j = 2m$ corresponds to the "retrograde corotation resonance," in which the particle moves at the corotation radius, but opposite to the body.[4]

### 3.4. Lindblad Resonances

Here, I restrict the term *Lindblad resonances* to first-order resonances ($j = 1$). In the literature, Equation (5) is usually written as $\kappa = \pm m(n - \Omega)$, with the convention $m > 0$. This introduces the presence of numerous $\pm$ and $\mp$ symbols in the equations, a possible source of errors. In contrast, taking both positive and negative values for $m$ eases the calculations by avoiding the cumbersome use of the $\pm$ symbol.

The various resonances described in this section are summarized in Figure 1 in a $(m, j)$ diagram.

## 4. Structure of Resonant Orbits

The potential $U(\mathbf{r})$ of Equation (2) can be expressed in terms of $\lambda'$ and $(a, e, \lambda, \varpi)$, and then expanded in powers of $e$ under the forms $r/a = 1 + \sum_{j=1}^{+\infty} e^j E_j \cos^j(\lambda - \varpi)$ and $L = \lambda + \sum_{j=1}^{+\infty} e^j L_j \sin^j(\lambda - \varpi)$, where $E_j$ and $L_j$ are numerical coefficients that describe the Keplerian motion. In doing so, each term $\cos(m\theta)$ in Equation (2), when combined to the terms $\cos^j$, $\sin^j(\lambda - \varpi)$, provides two terms of the form $e^j \cos[m\lambda' - (m - j)\lambda - j\varpi]$ and $e^j \cos[m\lambda' - (m + j)\lambda + j\varpi]$. Noting that the second term can be written $e^j \cos[(-m)\lambda' - (-m - j)\lambda - j\varpi]$, the expansion of $U(\mathbf{r})$ may be written using only terms of the form $m\lambda' - (m - j)\lambda - j\varpi$, where $m$ is positive or negative.

After reordering those terms, we obtain

$$
\begin{aligned}
U(\mathbf{r}) &= U(a, e, \lambda, \varpi, \lambda') \\
&= \sum_{k=-\infty}^{+\infty} U_k(a) \cos[k(\lambda - \lambda')] \\
&+ \sum_{m=-\infty}^{+\infty} \sum_{j=1}^{+\infty} \bar{U}_{m,j}(\alpha) e^j \cos[m\lambda' - (m - j)\lambda - j\varpi], \quad (11)
\end{aligned}
$$

where

$$
\alpha = \frac{a}{R}, \quad (12)
$$

$R$ being a characteristic dimension of the problem (to be defined later). Note that the first summation in Equation (11) describes the corotation resonance.

A given $m/(m - j)$ resonance occurs for $\nu_{m,j} = 0$, i.e., for $m\lambda' - (m - j)\lambda - j\varpi$ stationary. Let us denote $U_{m,j}$ the potential associated with that resonance, i.e.,

$$
U_{m,j}(a, e, \lambda, \varpi, \lambda') = \bar{U}_{m,j}(\alpha) e^j \cos(j\phi_{m,j}), \quad (13)
$$

where

$$
\phi_{m,j} = \frac{m\lambda' - (m - j)\lambda - j\varpi}{j} \quad (14)
$$

is the resonant argument. Note the dividing factor $j$, which ensures that the proper choice of canonical variables is made for use in the Hamiltonian describing the resonance (Peale 1986).

### 4.1. Resonance Order

The term $U_{m,j}$ is of order $e^j$, a property known as the d'Alembert's characteristic, and $j$ is called the order of the resonance.[5] The order $j$ is not entirely determined by the ratio $n/\Omega$, as the same value $n/\Omega = m/(m - j)$ can be achieved with multiples of $m$ and $j$. Let us denote $(m', j')$ the relatively prime (or irreducible) version of $(m, j)$. Then the same ratio $n/\Omega$ is achieved for all couples of the form $(km', kj')$, $k$ integer. Thus, at the same radius, an infinity of resonances of orders $j'$, $2j',\dots$ exist. Usually, only the resonance of lowest order, $j'$, is considered, and the higher order, weaker resonances are neglected.

The symmetry of the potential, however, may lead to the vanishing of some resonances. If the potential is invariant under a rotation of $2\pi/k$ radians (as is the case for normal sectoral modes in gaseous planets, for instance), then only $m_s'$ that are multiples of $k$ appear in Equation (2). Thus, the ratio $n/\Omega$ takes the form

$$
\frac{n}{\Omega} \sim \frac{m}{m - j} = \frac{kp}{kp - j}. \quad (15)
$$

Consequently, only $m/(m - j)$ resonances where $m$ is a multiple of $k$ survive in a $2\pi/k$-periodic potential. For instance, every other $k$ Lindblad resonance ($j = 1$) remains in this context. This is discussed in Section 5.2 with the potential of a triaxial ellipsoid, which is invariant under a $\pi$-rotation ($k = 2$). Then, only every other Lindblad resonance survives, those with even values of $m$, see Equation (27). Similarly, the second-

---

[4] The term retrograde corotation is in fact not appropriate because the particle mean motion does not match any harmonics of the potential. Actually, this resonance has the same dynamical behavior as the prograde 1/3 resonance, see Section 4.2. However, to keep in line with the nomenclature of other publications, I still use the term "retrograde corotation" in the text.

[5] Higher order terms in eccentricity are in fact present in the amplitude of the term $\cos(j\phi_{m,j})$, but they are ignored here.
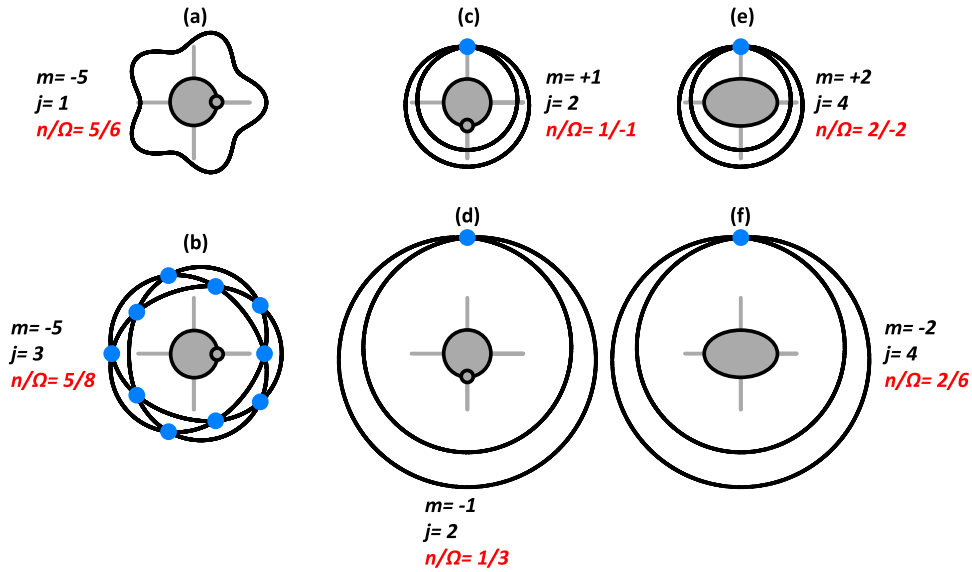
**Figure 2.** Pole-on view of various $m/(m-j)$ resonant periodic orbits around a body that is either a sphere with a mass anomaly sitting at its equator, or an elongated ellipsoidal object. The gray crosses correspond to the radius of the corotation orbit, where particles revolve at the same angular speed as the spin rate of the body. Each orbit has an eccentricity of 0.15. The blue dots mark the self-crossing points. (a) The periodic orbit corresponding to the 5/6 (first-order) outer Lindblad resonance. (b) The same for the 5/8 outer (third-order) resonance. The orbit has 3 braids, 5 identical sectors, and $|m|(j-1) = 10$ self-crossing points, thus satisfying Equation (17). (c) The retrograde "corotation" orbit, actually corresponding to the second-order retrograde resonance $1/-1$. (d) The true twin of Case (c), corresponding to the 1/3 outer resonance. The two orbits (c) and (d) have the same kinematics and same dynamical behaviors. They also are the only periodic orbits with a single self-crossing point ($|m'|(j'-1) = 1$). (e) The same as Case (c), but with an ellipsoidal central body. The resonance is now of order four and is labeled as $2/-2$. The cases (c) and (e) correspond to false twins, with the same kinematics but different orders, hence different dynamical behaviors. (f) The true twin orbit of Case (e), corresponding to the 2/6 fourth-order outer resonance.

order $1/3$ resonance vanishes, leaving the fourth-order $2/6$ resonances in its place. The distinction is important because, although corresponding to the same ratio $n/\Omega$, these two resonances have different phase portraits and different dynamical behaviors. To make that distinction clear, the $2/6$ notation should not be simplified to $1/3$.

### 4.2. Structure of the Periodic Resonant Orbits

Contrarily to the order, the kinematic structure of a resonant orbit depends only on the ratio $n/\Omega$, independently of the symmetry of the potential. The polar equation (in a frame rotating with the body) of a $m/(m-j)$ resonant periodic orbit is

$$\rho(\theta) = a\left[1 - e\cos\left(\frac{m}{j}\theta + \phi_{m,j}\right)\right].\qquad(16)$$

It can also be viewed as the polar equation of a perturbed streamline, where the particles move at different longitudes while sharing a common $\phi_{m,j}$. This aspect is discussed in Section 6. The structure of the periodic orbits is studied in detail in Sicardy et al. (2020). Noting again $(m', j')$ the irreducible version of $(m, j)$, results are (see also Figure 2):

1. The periodic orbit has $j'$ distinct braids.
2. The periodic orbit is invariant by a rotation of $2\pi/|m'|$, i.e., it possesses $|m'|$ identical sectors.
3. In each sector, the periodic orbit has $(j'-1)$ self-crossing points.

4. Thus, the total number of self-crossing points is[6]:

$$N_c = |m'|(j'-1).\qquad(17)$$

5. Consequently, Lindblad resonances ($j=1$) do not lead to self-crossing.[7]
6. The only resonances that result in a unique self-crossing point are for $|m'| = 1$ and $j' = 2$, corresponding to the second-order prograde $1/3$ and retrograde $1/-1$ resonances.
7. The lowest possible order of a retrograde resonance is $j' = 2$ (obtained with $m' = 1$ and $n/\Omega = 1/-1$). Thus, there are no retrograde Lindblad resonances.
8. Resonances having the same $|m'|$ and the same $j'$ correspond to orbits that have the same shape, and more precisely, that are homothetic. They have the same number of sectors, braids, and self-crossing points, i.e., they have the same kinematic behavior. I qualify two such resonances as *twins*. Note that twin resonances correspond to different ratios $|n/\Omega|$.
9. Two resonances that have the same $|m|$ and $j$ have not only the same kinematic behavior, but also the same order, i.e., the same dynamical behavior. I qualify two such resonances as *true twins* (while *false twins* are two resonances that have the same $|m'|$ and $j'$, but different $|m|$ and $j$). Example of true twins are the $1/3$ and $1/-1$ resonances mentioned above.[8] Figure 1 shows that any

---

[6] The eccentricity $e$ must be small enough to obtain only the essential self-crossing points, which are present even for vanishingly small eccentricities.

[7] The reciprocal is not true. For instance, the second-order $2/4$ resonant orbit has no self-crossing point, but it is not a Lindblad resonance.

[8] An example of a $1/-1$ resonance is the retrograde asteroid 2015 BZ$_{509}$ that shares Jupiter's orbit (Morais & Namouni 2017; Wiegert et al. 2017). An example of a $1/3$ resonance is given by the Trans-Neptunian Object (136120) 2003 LG$_7$ that completes one prograde orbit while Neptune completes three (https://minorplanetcenter.net/db_search/show_object?object_id=136120).

outer prograde resonance ($m < 0$) has a true twin that is either a retrograde (inner or outer) resonance, or an inner prograde resonance.

The same ratio $|n/\Omega|$, and thus the same orbital radius, corresponds to two different resonances, one prograde ($n/\Omega > 0$) and one retrograde ($n/\Omega < 0$). This is achieved for pairs of ($m'_p$, $j'_p$) and ($m'_r$, $j'_r$), satisfying $m'_p/(m'_p - j'_p) = -m'_r/(m'_r - j'_r)$, where the subscripts "p" and "r" refer to prograde and retrograde motions, respectively. The couples ($m'_p$, $j'_p$) and ($m'_r$, $j'_r$) are each irreducible, so are both couples ($m'_p$, $m'_p - j'_p$) and ($m'_r$, $m'_r - j'_r$). Gauss' theorem thus implies that $|m'_r| = |m'_p|$. More precisely, since $m'_r > 0$ (Figure 1), we must have $m'_r = |m'_p|$. Distinguishing the cases $m'_p = m'_r$ and $m'_p = -m'_r$, accounting for the fact that $m'_p < 0$ or $m'_p > j'_p$ (Equation (10)) and that $j'_p, j'_r > 0$ by convention, it is easy to show that if $m'_p < 0$, then $m'_r = -m'_p$ and $j'_r = j'_p - 2m'_p$, while if $m'_p > j'_p$, then $m'_r = m'_p$ and $j'_r = 2m'_p - j'_p$.

In all cases, $j'_r > j'_p$. Thus, at a given orbital radius, retrograde resonances are always of higher order than prograde resonances, a result already found by Morais & Giuppone (2012). For instance, the 3/2 prograde resonance is of order one ($m' = 3, j' = 1$), while the 3/−2 retrograde resonance is of order five ($m' = 3, j' = 5$).

## 5. Resonance Strength

We now calculate the terms $\bar{U}_{m,j}(\alpha)$ of Equation (11), first in the case of a mass anomaly, and then generalizing the results to any potential of the form of Equation (2).

### 5.1. Mass Anomaly

We consider a spherical body of mass $M$ and radius $R$, with a mass anomaly $m_a$ sitting on its equator. The potential $U(\boldsymbol{r})$ then takes the form (Sicardy et al. 2019)

$$U(\boldsymbol{r}) = -\frac{GM}{r} - \frac{GM\mu}{R}$$
$$\times \left\{ \frac{1}{2}\sum_{m=-\infty}^{+\infty}\left[ b_{1/2}^{(m)}\left(\frac{r}{R}\right) - q\delta_{(|m|,1)}\left(\frac{r}{R}\right)\right]\cos(m\theta)\right\},$$
$$(18)$$

where $q = \Omega^2 R^3/GM$ is the rotation parameter, $\mu = m_a/M$ is the normalized mass anomaly, $b_{1/2}^{(m)}$ is the classical Laplace coefficient $b_{\gamma}^{(m)}(\alpha) = (2/\pi)$ $\int_0^\pi \cos(m\theta)/[1 + \alpha^2 - 2\alpha\cos(\theta)]^\gamma \, d\theta$, and the symbol $\delta_{(|m|,1)}$ is the Kronecker delta function stemming from the indirect part of the potential in $U(\boldsymbol{r})$, while the terms $b_{1/2}^{(m)}$ describe the direct part of the potential. This potential is formally identical to that caused by a satellite on a circular orbit (corresponding to $q = 1$), except that the mass anomaly revolves at angular velocity $\Omega$ (instead of the Keplerian velocity of a satellite) at the surface of the body. This effect is encapsulated in the parameter $q$.

The coefficients $\bar{U}_{m,j}(\alpha)$ are calculated using the formal expansions of the disturbing potential due to a satellite on a circular orbit, see MD00/EM00. For instance, consider the

first-order resonant argument $\phi_{m,1} = m\lambda' - (m-1)\lambda - \varpi$ with $m > 0$ corresponding to an external perturber. The aforementioned references then provide[9]

$$\bar{U}_{m,1}(\alpha) = -\frac{GM\mu}{R}f_{27}, \qquad (19)$$

where

$$f_{27} = \frac{1}{2}[-2m - \alpha D][b_{1/2}^{(m)}(\alpha) - q\delta_{(|m|,1)}\alpha], \text{ with } D = \frac{d}{d\alpha}. \qquad (20)$$

The factor $f_{27}$ can be rewritten

$$f_{27} = F_{27}[b_{1/2}^{(m)}(\alpha) - q\delta_{(|m|,1)}\alpha], \qquad (21)$$

where $F_{27} = (1/2)[-2m - \alpha D]$ is now a linear operator. Note that we have included here the *indirect part of the potential*, $q\alpha\delta_{|m|,1}$. It is easy to verify that the operator $F_n$ can be generically applied to that indirect term, so that there is no need to look at the entries of the indirect parts in the tables.[10] Actually, since the indirect part of the potential is linear in $\alpha$, the differential operators $D^p = d^p/d\alpha^p$ applied to the indirect term reduce the simple form

$$\alpha^p D^p = \alpha\delta_{(p,1)}. \qquad (22)$$

For $m < 0$, then the factor usually considered in Equation (19) is $f_{31}$ instead of $f_{27}$. However, this complication is not necessary, as $f_{31}$ is a mere avatar of $f_{27}$, that can be deduced from it through the transformation $m \to 1 - m$ and $\alpha \to 1/\alpha$. Note that in doing so, we may have $\alpha > 1$. This poses a priori a problem from a computational point of view, as classical series expansions of $b_{1/2}^{(m)}(\alpha)$ use series in powers of $\alpha$ that converge only for $\alpha < 1$. However, this problem is easily resolved by using the identity $b_{1/2}^{(m)}(\alpha) = b_{1/2}^{(m)}(1/\alpha)/\alpha$.

The same approach can be used for any resonance $m/(m - j)$, considering only the entries with cosine arguments of the form $m\lambda' - (m - j)\lambda - \varpi$ in order to find $F_n$ (in practice, the entries labeled "4D$j$.1" in MD00/EM00). Then the fact that the perturber is internal or external is automatically accounted for through the values of $m$ and $j$. So, the term $U_{m,j}(\alpha)$ in Equation (13) is given by

$$\bar{U}_{m,j}(\alpha) = F_n\left[-\left(\frac{GM\mu}{R}\right)[b_{1/2}^{(m)}(\alpha) - q\delta_{(|m|,1)}\alpha]\right]. \qquad (23)$$

Comparing Equations (2) and (18), from the unicity of the Fourier expansion, and from the linearity of the operators $F_n$, we finally obtain for a generic potential as given by Equation (2)

$$\bar{U}_{m,j}(\alpha) = 2F_n[U_m(\alpha)]. \qquad (24)$$

This is the central equation of this section, as it gives the amplitude $\bar{U}_{m,j}(\alpha)$ of any $m/(m - j)$ resonance term, whether internal or external, and whether direct or indirect in nature, and for any potential of the form of Equation (2), i.e., satisfying the conditions (i)–(iii) at the start of Section 2. As a word of caution, note that if Equation (1) is used instead of

---

[9] Note that MD00/EM00 denote the azimuthal number $j$, while we use $m$ here.
[10] This point is mentioned in Agnor & Lin (2012, p. 6).

**Table 1**
Resonant Terms $\bar{U}_{m,j}(\alpha)$ (Equation (13))

| Order $j$ | $\bar{U}_{m,j}$ | Operators $F_n$ (Equation (24)) |
|---|---|---|
| 1 | $2eF_{27}[U_m(\alpha)]\cos(\phi_{m,1})$ | $F_{27} = (1/2)[-2m - \alpha D]$ (Lindblad resonances) |
| 2 | $2e^2F_{45}[U_m(\alpha)]\cos(2\phi_{m,2})$ | $F_{45} = (1/8)[-5m + 4m^2 + (-2 + 4m)\alpha D + \alpha^2 D^2]$ |
| 3 | $2e^3F_{82}[U_m(\alpha)]\cos(3\phi_{m,3})$ | $F_{82} = (1/48)[-26m + 30m^2 - 8m^3 + (-9 + 27m - 12m^2)\alpha D$ |
|  |  | $\quad + (6 - 6m)\alpha^2 D^2 - \alpha^3 D^3]$ |
| 4 | $2e^4F_{90}[U_m(\alpha)]\cos(4\phi_{m,4})$ | $F_{90} = (1/384)[-206m + 283m^2 - 120m^3 + 16m^4$ |
|  |  | $\quad + (-64 + 236m - 168m^2 + 32m^3)\alpha D$ |
|  |  | $\quad + (48 - 78m + 24m^2)\alpha^2 D^2 + (-12 + 8m)\alpha^3 D^3 + \alpha^4 D^4]$ |

**Note.** The operators $F_n$ are found in Murray & Dermott (2000) or Ellis & Murray (2000). The resonant argument $\phi_{m,j}$ is given in Equation (14) and $D$ is the radial derivative operator, $D = d/d\alpha$. When applied to indirect terms, $\alpha^p D^p = \alpha\delta_{(p,1)}$ (Equation (22)). In the case of a homogeneous triaxial ellipsoid, the operator $\alpha^p D^p$ reduces to a multiplicative factor $\alpha^p D^p = (-1)^p(|m| + 1)...(|m| + p)$ (Equation (31)).

Equation (2), then we must use $\bar{U}_{m,j}(\alpha) = F_n[U_m(\alpha)]$ instead of Equation (24).

The operators $F_n$ for resonances of order 1, 2, 3, and 4 are listed in Table 1.

### 5.2. Triaxial Homogeneous Ellipsoid

We now consider the example of a triaxial homogeneous ellipsoid with semiaxes $A > B > C$, rotating around its minor axis $C$, see details in Sicardy et al. (2019, 2020). The reference radius $R$ of the ellipsoid is defined by

$$\frac{3}{R^2} = \frac{1}{A^2} + \frac{1}{B^2} + \frac{1}{C^2}, \tag{25}$$

and its elongation and oblateness are measured by the dimensionless parameters $\epsilon$ and $f$

$$\epsilon = \frac{A^2 - B^2}{2R^2} \quad \text{and} \quad f = \frac{A^2 + B^2 - 2C^2}{4R^2}. \tag{26}$$

Because of the symmetry of the body, its potential is invariant under a $\pi$-rotation, so that only even values of $m$ appear in the Fourier expansion in Equation (2), thus eliminating the indirect part of the potential. Posing $m = 2p$, the resonance condition (7) now reads

$$\frac{n}{\Omega} \sim \frac{2p}{2p - j}, \tag{27}$$

which eliminates (among others) every other Lindblad resonances, keeping only those with $m$ even. For instance, the 4/3 resonance ($m = 4$, $j = 1$) survives as a Lindblad resonance, while the 5/4 resonance vanishes, leaving its place to the second-order resonance 10/8 resonance ($m = 10, j = 2$).

At lower order in $\epsilon$ and $f$, $U(\boldsymbol{r})$ is given by Sicardy et al. (2019, 2020)

$$U(\boldsymbol{r}) = -\frac{GM}{R} \sum_{m=-\infty}^{+\infty} \left(\frac{R}{r}\right)^{|m|+1}$$
$$\times \epsilon^{|m/2|}S_{|m/2|}\cos(m\theta) \quad (m \text{ even}), \tag{28}$$

where $S_{|p|}$ is recursively defined by

$$S_{|p|+1} = 2\frac{(|p| + 1/4)(|p| + 3/4)}{(|p| + 1)(|p| + 5/2)} \times S_{|p|} \quad \text{with} \quad S_0 = 1. \tag{29}$$

By comparing Equations (2) and (28), we obtain

$$U_m(\alpha) = -\left(\frac{GM}{R}\right)\frac{\epsilon^{|m/2|}S_{|m/2|}}{\alpha^{|m|+1}} \quad (m \text{ even}), \tag{30}$$

where again $\alpha$ is given by Equation (12). Due to the form of $U_m(\alpha)$, a power of $\alpha$, the differential operator $\alpha^p D^p$ reduces here to a mere multiplicative factor

$$\alpha^p D^p = (-1)^p(|m| + 1)...(|m| + p) \quad (m \text{ even}), \tag{31}$$

so that the operators $F_n$ in Table 1 are multiplicative factors that are polynomial functions of $m$ and $|m|$. From Equation (24),

$$\bar{U}_{m,j}(\alpha) = -\left(\frac{GM}{R}\right)\epsilon^{|m/2|}\left(\frac{2S_{|m/2|}F_n}{\alpha^{|m|+1}}\right)$$
$$\times e^j\cos(j\phi_{m,j}) \quad (m \text{ even}), \tag{32}$$

This is a convenient way to express $\bar{U}_{m,j}(\alpha)$ as the product of

1. A potential term $-GM/R$ that globally scales the problem in terms of mass and length.
2. A dimensionless term $\epsilon^{|m/2|}$ that measures the departure of the body from axisymmetry (akin to a mass anomaly).
3. A dimensionless factor $2S_{|m/2|}F_n/\alpha^{|m|+1}$ that is intrinsic to the resonance, i.e., to the azimuthal number $m$ (Table 1) and the order $j$, through the value of $\alpha$.
4. A term $e^j$ that defines the resonance order.
5. A trigonometric term $\cos(j\phi_{m,j})$, where $\phi_{m,j}$ is defined by Equation (14).

In order to isolate what is intrinsic to the resonance geometry and to the nonaxisymmetry of the body, I define the strength of a $m/(m - j)$ resonance as the dimensionless coefficient

$$\mathfrak{S}_{m,j} = \epsilon^{|m/2|}\left(\frac{2S_{|m/2|}F_n}{\alpha^{|m|+1}}\right) \quad (m \text{ even}). \tag{33}$$

The factors $F_n$ are given in Table 1 and $S_{|m/2|}$ is defined in Equation (29). The factor $\alpha$ can be calculated from the condition $j\kappa(a) = m[n(a) - \Omega]$ and the expressions of $n(a)$ and $\kappa(a)$ as a function of $GM$, $\epsilon$ and $f$. To lowest order in $\epsilon$ and $f$, we

**Table 2**
Resonance Strengths Around Homogenous Ellipsoids

| m→ | Azimuthal Number | | | | | | | |
|---|---|---|---|---|---|---|---|---|
| | −8 | −6 | −4 | −2 | 2 | 4 | 6 | 8 |
| Order $j\downarrow$ | | | | Chariklo[a] | | | | |
| 1 | $0.0105\epsilon^4 e$ 210 [8/9] | $0.0207\epsilon^3 e$ 214 [6/7] | $0.0439\epsilon^2 e$ 223 [4/5] | $0.102\epsilon e$ 250 [2/3] | inside [2/1] | $-0.0408\epsilon^2 e$ 169 [4/3] | $-0.0200\epsilon^3 e$ 178 [6/5] | $-0.0103\epsilon^4 e$ 182 [8/7] |
| 2 | **** 223 [8/10] | $0.0641\epsilon^3 e^2$ 232 [6/8] | **** 250 [4/6] | $0.143\epsilon e^2$ 300 [2/4] | apsidal [2/0] | **** [4/2] | $0.0336\epsilon^3 e^2$ 160 [6/4] | **** 169 [8/6] |
| 3 | $0.125\epsilon^4 e^3$ 237 [8/11] | **** 250 [6/9] | $0.185\epsilon^2 e^3$ 275 [4/7] | $0.190\epsilon e^3$ 348 [2/5] | inside [2/−1] | inside [4/1] | **** [6/3] | inside [8/5] |
| 4 | **** 250 [8/12] | $0.331\epsilon^3 e^4$ 267 [6/10] | **** 300 [4/8] | $0.251\epsilon e^4$ 392 [2/6] | $0.00251\epsilon e^4$ 196 [2/−2] | **** [4/0] | inside [6/2] | **** [8/4] |
| Order $j\downarrow$ | | | | Haumea[b] | | | | |
| 1 | $0.0163\epsilon^4 e$ 1238 [8/9] | $0.0294\epsilon^3 e$ 1263 [6/7] | $0.0570\epsilon^2 e$ 1313 [4/5] | $0.121\epsilon e$ 1463 [2/3] | inside [2/1] | inside [4/3] | inside [6/5] | inside [8/7] |
| 2 | **** 1313 [8/10] | $0.0937\epsilon^3 e^2$ 1363 [6/8] | **** 1463 [4/6] | $0.171\epsilon e^2$ 1752 [2/4] | apsidal [2/0] | **** [4/2] | inside [6/4] | **** [8/6] |
| 3 | $0.204\epsilon^4 e^3$ 1388 [8/11] | **** 1463 [6/9] | $0.248\epsilon^2 e^3$ 1609 [4/7] | $0.229\epsilon e^3$ 2025 [2/5] | inside [2/−1] | inside [4/1] | **** [6/3] | inside [8/5] |
| 4 | **** 1463 [8/12] | $0.500\epsilon^3 e^4$ 1561 [6/10] | **** 1752 [4/8] | $0.302\epsilon e^4$ 2285 [2/6] | $0.00286\epsilon e^4$ 1164 [2/−2] | **** [4/0] | inside [6/2] | **** [8/4] |

**Notes.** In each box, the factor $\mathfrak{S}_{m,j}e^j$ is calculated for the specified values of $m$ and $j$, using Equation (33). Below each factor are the corresponding resonant radius (km) and the ratio $[n/\Omega]$. The term "inside" means that the resonance formally occurs inside the physical volume of the body, and is thus unphysical. Note that the apsidal resonances also occur formally inside the body, and are not treated here. The **** symbols indicate resonances that are already listed elsewhere in the table under a lower order version, see the text.
[a] Using $M = 6.3 \times 10^{18}$ kg, $T_{rot} = 2\pi/\Omega = 7.004$ hr, $A \times B \times C = 57 \times 139 \times 86$ km, $R = 115$ km, $f = 0.20$, $\epsilon = 0.61$ (Leiva et al. 2017).
[b] Using $M = 4.006 \times 10^{21}$ kg, $T_{rot} = 3.915341$ hr, $A \times B \times C = 1161 \times 852 \times 513$ km, $R = 712$ km, $f = 0.55$, $\epsilon = 0.76$ (Ortiz et al. 2017).

have from Equation (8) and Sicardy et al. (2019, 2020)[11]

$$n^2(r) \sim \frac{GM}{a^3}\left[1 + \frac{3f}{5}\left(\frac{R}{a}\right)^2\right] \text{ and }$$

$$\kappa^2(r) \sim \frac{GM}{a^3}\left[1 - \frac{3f}{5}\left(\frac{R}{a}\right)^2\right], \tag{34}$$

and $\alpha = a/R$ can be numerically determined through an iterative process if $f$ is sufficiently small, see, e.g., Renner & Sicardy (2006).

As examples, the factors $\mathfrak{S}_{m,j}e^j$ are listed in Table 2 in the cases of Chariklo and Haumea, assumed to be homogeneous triaxial bodies. The following points can be noted:

1. Because of the term $\epsilon^{|m/2|}$, the resonance strength rapidly tends to zero as $m$ tends to infinity, i.e., as one approaches the corotation radius, see an example in Figure 2 of Sicardy et al. (2019). This contrasts with the case of a perturbing satellite, for which $\mathfrak{S}_{m,j}$ increases as $m$ increases (for $j$ fixed), since the particles orbit closer and closer to the satellite.

2. Some resonances are not replicated Table 2 (symbols ****) because only the lowest order in eccentricity has been considered for a given ratio $n/\Omega$. For instance, the $m = -2$, $j = 2$ case, corresponding to the second-order

---

[11] If need be, higher order terms in $f$ and $\epsilon$ can be introduced in Equation (34), using the expansions of Sicardy et al. (2019, 2020).

$\epsilon e^2$-resonance $(n/\Omega = 2/4)$, is not considered in its fourth-order version $\propto \epsilon^2 e^4$ with $m = -4$, $j = 4$ $(n/\Omega = 4/8)$.

## 6. Concluding Remarks

In this paper, I have investigated the structure of the $j\kappa = m(n - \Omega)$ sectoral resonances in the equatorial plane of a nonaxisymmetric object rotating at rate $\Omega$. The cases $j = 0$ (corotation) and $m = j$ (apsidal) are not studied here. Figure 1 summarizes the general taxonomy for those resonances and Figure 2 illustrates some of the results on the structure of resonant orbits.

The kinematic structure of a resonant orbit associated with $(m, j)$ is entirely encapsulated in the couple $(m', j')$, the irreducible (relatively prime) version of $(m, j)$. Thus, the kinematic structure of the orbit only depends on $n/\Omega \sim m/(m - 1) = m'/(m' - j')$, i.e., on the resonance location, and is independent of the nature of the potential. More precisely, the resonant orbit has $j'$ braids, $|m'|$ identical sectors, and $|m'|(j' - 1)$ self-crossing points.

The existence of a resonance, and therefore its order $j$ for a given $n/\Omega$ ratio, depends on the symmetry of the potential. In particular, a potential that is invariant under a $2\pi/k$-rotation creates only resonances of the form $kp/(kp - j)$. This is why, for instance, the second-order 1/3 resonance around a spherical body with a mass anomaly, which has $m = -1$, $j = 2$, $k = 1$,

is replaced by the fourth-order resonance 2/6 around a homogeneous ellipsoid, which has $m = -2$, $j = 4$, $k = 2$.

Resonances that have opposite $m$ and the same $j$ have periodic orbits that possess the same kinematic structure and the same order, i.e., the same dynamical behavior. Here, they are called *true twin* resonances. Resonances with opposite $m'$ and the same $j'$, but different $|m|$ and $j$ are called *false twin* resonances, because they correspond to the same kinematic, but to different dynamical, behaviors.

A retrograde resonance ($n/\Omega < 0$) is always of higher order than the corresponding prograde resonance occurring at the same radius, but with $n/\Omega > 0$. This shows that there are no retrograde Lindblad ($j = 1$) resonances.

The resonance strengths can be calculated using a unique operator (for a given couple $(m, j)$) that acts on the direct and indirect parts of the potential, and that is valid for inner, outer, prograde, and retrograde resonances, see Equation (24). These operators are in fact the classical operators $F_n$ used for satellite perturbations. In the case of a homogeneous triaxial ellipsoid, they reduce to mere multiplicative factors (Table 1) that are easily implemented in numerical schemes. Examples are given in Table 2 for Chariklo and Haumea, assumed to be homogeneous triaxial ellipsoids.

This study is intended to be general enough to serve in a broad range of contexts. For instance, the results can easily be generalized in cases where the central body has several equatorial mass anomalies. Then, it is enough to split the potential in elementary, single-anomaly potentials, and accounting for the fact that those potentials are out of phase.

As mentioned earlier, Equation (16) can be seen as describing a streamline of particles in a collisional disk. Then difficulties arise because self-crossing causes singularities in the hydrodynamical equations that describe the flow of particles near the resonance. Moreover, and except for the Lindblad resonances, these equations involve nonlinear perturbations because they are of order $j > 1$ in eccentricity, a further source of complications.

However, not having the appropriate hydrodynamical equations does mean that those resonances have no effect on the disk. In that context, it would be interesting to use works already done on granular flows or kinetic theories to describe neighbor-streamline crossings in waves excited by Lindblad resonances, see, e.g., Borderies et al. (1985) and Shu et al. (1985). Another approach is to rely on collisional codes that include a realistic description of particulate collisions in rings. This can be relevant to Chariklo's and Haumea's rings, as both ring systems are found to orbit near the second-order 1/3 (or fourth-order 2/6) resonance with their host body (Ortiz et al. 2017; Sicardy et al. 2020), a subject of future works.

## ORCID iDs

Bruno Sicardy ⓘ https://orcid.org/0000-0003-1995-0842

## References

Agnor, C. B., & Lin, D. N. C. 2012, ApJ, 745, 143
Borderies, N., Goldreich, P., & Tremaine, S. 1985, Icar, 63, 406
Braga-Ribas, F., Sicardy, B., Ortiz, J. L., et al. 2014, Natur, 508, 72
Chandrasekhar, S. 1942, Principles of Stellar Dynamics (Chicago, IL: Univ. Chicago Press)
Ellis, K. M., & Murray, C. D. 2000, Icar, 147, 129
Leiva, R., Sicardy, B., Camargo, J. I. B., et al. 2017, AJ, 154, 159
Morais, H., & Namouni, F. 2017, Natur, 543, 635
Morais, M. H. M., & Giuppone, C. A. 2012, MNRAS, 424, 52
Murray, C. D., & Dermott, S. F. 2000, Solar System Dynamics (Cambridge: Cambridge Univ. Press)
Ortiz, J. L., Santos-Sanz, P., Sicardy, B., et al. 2017, Natur, 550, 219
Peale, S. J. 1986, in Satellites, ed. J. A. Burns & M. S. Matthews (Tucson, AZ: Univ. Arizona Press), 159
Pfenniger, D. 1984, A&A, 134, 373
Renner, S., & Sicardy, B. 2006, CeMDA, 94, 237
Scheeres, D. J. 1994, Icar, 110, 225
Shu, F. H., Dones, L., Lissauer, J. J., Yuan, C., & Cuzzi, J. N. 1985, ApJ, 299, 542
Sicardy, B., Leiva, R., Renner, S., et al. 2019, NatAs, 3, 146
Sicardy, B., Renner, S., Leiva, R., et al. 2020, in The Trans-Neptunian Solar System, ed. D. Prialnik, M. A. Barucci, & L. A. Young (Amsterdam: Elsevier), 249
Wiegert, P., Connors, M., & Veillet, C. 2017, Natur, 543, 687